Journal of the European Ceramic Society 16 (1996) 627–635

0955-2219(95)00179-4
0955-2219/96/$15.00

Sintering Behaviour of Precursor Mullite Powders and Resultant Microstructures

F. Kara* & J. A. Little

Department of Materials Science and Metallurgy, University of Cambridge, Cambridge CB2 3QZ, UK

(Received 5 April 1995; revised version received 14 September 1995; accepted 29 September 1995)

Abstract

Crystallization and sintering behaviour of two structurally different diphasic precursor mullite powders were studied. Powder derived from boehmite and colloidal silica formed mullite at around 1250°C and could be sintered to high density at this temperature by viscous flow sintering. Calcination of the powder up to 1000°C did not affect its sinterability but the weight loss decreased from 20% for the uncalcined powder to 5% for the 1000°C calcined powder. In contrast, powder derived from aluminium sulfate and colloidal silica formed mullite at around 1200°C and did not sinter much by the viscous flow, but showed enhanced solid-state sintering behaviour compared with crystalline mullite powders. Calcination of the powder at temperatures below mullite formation temperature did not affect its sinterability. Microstructural examinations revealed that dense mullite obtained by sintering of powder derived from aluminium sulfate–colloidal silica had much finer grain size (~135 nm) than that obtained from the boehmite–colloidal silica mixture (~1500 nm) and the fine grain size of the mullite was stable up to 1300°C upon long heat treatments (120 h).

1 Introduction

Although it has long been known in refractories, mullite has recently also emerged as an important ceramic material for electronic, optical and high-temperature structural applications owing to its attractive properties such as high creep resistance, retention of strength up to high temperatures, low thermal expansion, density and dielectric constant, and infra-red transparency at medium wavelengths.

Dense mullite ceramics can be produced by various methods including reaction sintering of alumina–silica mixtures and solid-state sintering of fine crystalline mullite powders. Fine crystalline mullite powder compacts require high temperatures (≥1600°C) to enable them to be sintered to high density. This is due to the low inter-diffusion rates of aluminium and silicon ions in mullite.[1] Reaction sintering temperatures of mullite precursors vary depending on the scale of mixing.

(a) Micrometre-scale alumina–silica mixtures require temperatures >1600°C for sintering and mullite formation.[2]

(b) Mixtures of fine α-Al_2O_3 and amorphous silica can be sintered to full density at ~1300°C by viscous flow of the amorphous phase. Completion of mullite formation in these mixtures in a reasonable time requires temperatures of ~1600°C.[3,4]

(c) Similarly, gels prepared from nanometre-scale (diphasic) mixtures of alumina and silica (e.g. a mixture of boehmite (AlOOH) and colloidal silica) can also be sintered to almost full density at ~1250°C by the viscous flow. However, conversion to mullite can be achieved at much lower temperatures than α-Al_2O_3–silica mixtures (1300–1350°C)[5–8] due to the finer scale of mixing of the diphasic mixtures.

Due to the intrinsic presence of crystal water, gels or powders that are prepared by using boehmite undergo large weight losses due to the decomposition of boehmite above 400°C. Such large weight losses have been observed to cause cracking of small pellets[9] and in sintering of large compacts this would be an even greater problem. In addition, the heating rate would have to be slow during sintering. Therefore, the calcination of the powders above the boehmite decomposition temperature becomes necessary to reduce weight losses. Calcination at high temperatures may also decrease the surface area of the powders which improves their processability.

In this study, two types of diphasic powders, varying in the size of the alumina component, were prepared from boehmite–colloidal silica and

*Now with Anadolu Üniversitesi, Yunusemre Kampüsü, Seramik Müh. Böl., 26470 Eskisehir, Turkey.

aluminium sulfate–colloidal silica mixtures. Their crystallization behaviour, powder characteristics, sintering behaviour after calcination at various temperatures and microstructures were studied and compared.

2 Experimental

Mullite precursor powders were produced from two different aluminium sources by the sol–gel method. A commercial pseudoboehmite powder (Cerasol, AlOOH, 99·96%, BA Chemicals, Buckinghamshire, UK) and aluminium sulfate [$Al_2(SO_3)_3 \cdot 16$–$18H_2O$, 99·4%, BDH Chemicals, Poole, UK] were used as the alumina source. The silica source was high purity colloidal silica (BDH Chemicals, Poole, UK).

Powder A was prepared from pseudoboehmite (surface area of 170 $m^2\ g^{-1}$) and colloidal silica (surface area of 200 $m^2\ g^{-1}$). An AlOOH sol was obtained by dispersing the boehmite powder in water for 0·5 h. The pH of the as-dispersed sol was 3·4. A silica sol was prepared by dispersing the colloidal (or fumed) silica powder in water for 0·5 h at pH 7 (adjusted by NH_4OH). The silica sol was added into the AlOOH sol under vigorous mixing by a high speed mixer and mixing was continued for 0·5–1 h. The mixture was kept in an oven at 60–80°C for gelation and drying. The dried gel fragments were crushed and ground by a motor-driven pestle and mortar, calcined at 550 and 1000°C for 2 h and then milled in methanol using ZrO_2 or alumina balls in polyethylene jars. Milling by ZrO_2 or alumina balls did not cause any detectable contamination [verified by electron probe microanalysis (EPMA) (SX50 Cameca)] or changes in the microstructure. The drying of the milled powder was carried out in an oven at 80°C.

Powder B was prepared from aluminium sulfate and colloidal silica. The alumina sol was prepared by dissolving aluminium sulfate in water. The pH in the as-dissolved condition was 2·2. The silica sol (pH 7) was then added into the alumina sol under vigorous mixing. The mixture was kept in an oven at 125°C for gelation and drying. The gel fragments were then crushed and ground by the motor-driven pestle and mortar and calcined at high temperatures (>850°C) to decompose the aluminium sulfate. Powder B was milled under the same conditions as powder A.

The sintering experiments were carried out by pressing powders into pellets (10 or 13 mm in diameter) in a die at 100 MPa which were then isopressed at 450 MPa. No pressing aid was used. All the sintering experiments were done in still air and the heating rate during sintering was 5°C min^{-1}.

The surface area and particle size of the powders were measured by the BET method using nitrogen gas absorption (Micromeritics Asap 2000) and a laser diffraction particle size analyser (Malvern, Master Sizer), respectively. The Al_2O_3/SiO_2 ratio of the sintered compacts was obtained by EPMA.

The crystallization behaviour of both powders was studied by X-ray diffraction (Philips PW 3719) after calcining them at various temperatures for a constant time.

Green and sintered densities were measured from the dimensions of the as-pressed pellets and by the water immersion technique based on Archimedes' principle, respectively. At least three samples were measured and an average was taken. Relative bulk densities were calculated by taking the theoretical density of mullite as 3·17 g cm^{-3} (JCPDS Card No: 15-776) . The difference between the relative densities of the pellets which were treated under the same conditions was always <0·5% and mostly <0·2%.

Microstructural examinations were carried out by transmission electron microscopy [(TEM) Philips 400ST].

3 Results and Discussion

Since mullite is a solid solution of alumina and silica, the production of mullite free from defects (e.g. glassy phase, cristobalite or alumina) from aluminium- and silicon-bearing compounds requires the mixing of these homogeneously. Homogeneous mixing between boehmite and silica sols can be obtained by heterocoagulation. Heterocoagulation is achieved by the preparation of stable sols of alumina and silica with opposite surface charges (ζ potential). AlOOH particles at pH 3·4 and silica particles at pH 7 bear a net positive and negative surface charge, respectively,[10] and thus mixing of these should result in maximum contact between boehmite and silica particles.

The particle size of boehmite calculated from its surface area (170 $m^2\ g^{-1}$, given by the supplier) was ~12 nm while TEM examination showed it to be ~20 nm. The particle size of colloidal silica calculated from its measured surface area (200 $m^2\ g^{-1}$) was 14 nm. Therefore, when positively charged boehmite particles are mixed with negatively charged silica particles, the silica particles are expected to surround the boehmite particles, as in Fig. 1(a).

In the case of powder B, the situation is slightly different. When aluminium sulfate is dissolved in water, it undergoes hydrolysis and condensation reactions. Under the acidic conditions (pH 2), which are used here, the condensation reactions

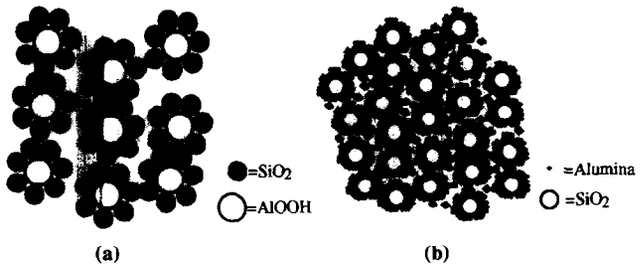

Fig. 1. Schematic representation of the expected particle arrangement of alumina and silica when (a) boehmite and (b) aluminium sulfate is used as the alumina source.

are suppressed while the hydrolysis reactions are dominant.[11] Therefore, the alumina particles derived from aluminium sulfate should be much smaller than the boehmite particles. Therefore, the mixing of the alumina sol from aluminium sulfate with the silica sol should result in the surrounding of silica particles with the aluminium oxide particles, as in Fig. 1(b).

The alumina content of mullite derived from both powders, measured by EPMA, was 72·2 wt%.

3.1 Crystallization

The development of crystalline phases from the AlOOH and colloidal silica mixture (powder A) on heating is shown in the corresponding X-ray traces in Fig. 2. At 1225°C after 2 h, the main phases present were δ-Al_2O_3 and an amorphous phase (a broad peak at around $2\theta = 20°$). After 2 h at 1250°C, the formation of mullite took place from the reaction between δ-Al_2O_3 and the amorphous phase. Although not shown in Fig. 2, the formation of mullite was not observed after 15 min at 1250°C. This indicates that mullite formation occurred after an incubation period as pointed out by others.[12–14] The incubation period was the time taken for the dissolution of transitional alumina into the amorphous phase (from which mullite nucleates[15]) to reach the critical nucleation concentration.[12,14,15] After 1300°C for 2 h, the extent of mullite formation increased with the consumption of δ-Al_2O_3 and amorphous silica but some θ-Al_2O_3 was still present. The presence of θ-Al_2O_3 together with mullite is attributed to large boehmite particles (or undispersed boehmite agglomerates) present in the starting materials which were not able to react at short times. On further heating to 1420°C for 5 h, the only crystalline phase present was mullite. The crystallization of mullite without the individual crystallization of α-Al_2O_3 and/or cristobalite indicates that the mixing method employed provided a very good degree of mixing between boehmite and silica particles.

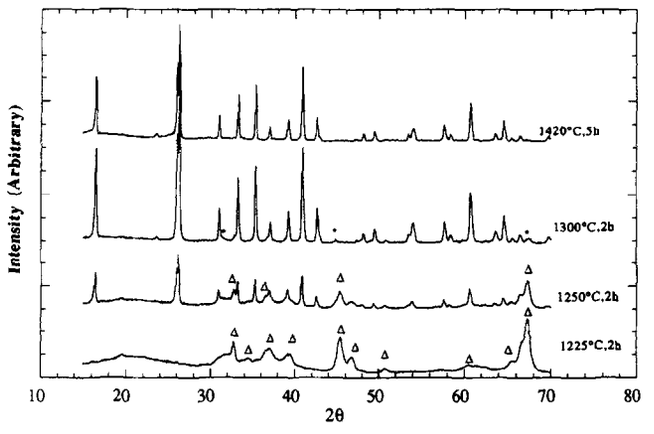

Fig. 2. Development of crystallization of powder A. (Δ) δ-Al_2O_3, (*) θ-Al_2O_3. Some of the δ-Al_2O_3 peaks at 1250°C are not labelled. Mullite peaks are not labelled.

Figure 3 shows TEM defocus images of a powder A compact sintered at 1250°C for 2 h. The amorphous phase, which shows bright contrast when imaged under-focus, was distributed homogeneously in the microstructure and surrounded the δ-Al_2O_3 particles. (An amorphous low density phase shows bright and dark contrast in under-focus and over-focus conditions, respectively.[16]) This further confirms that the processing conditions resulted in homogeneous mixing.

The development of crystallization of powder B has been reported earlier.[17] A large amount of mullite formation was observed at 1200°C in the presence of γ-Al_2O_3 type spinel and an amorphous phase. The formation of δ-Al_2O_3 and θ-Al_2O_3 was not observed.

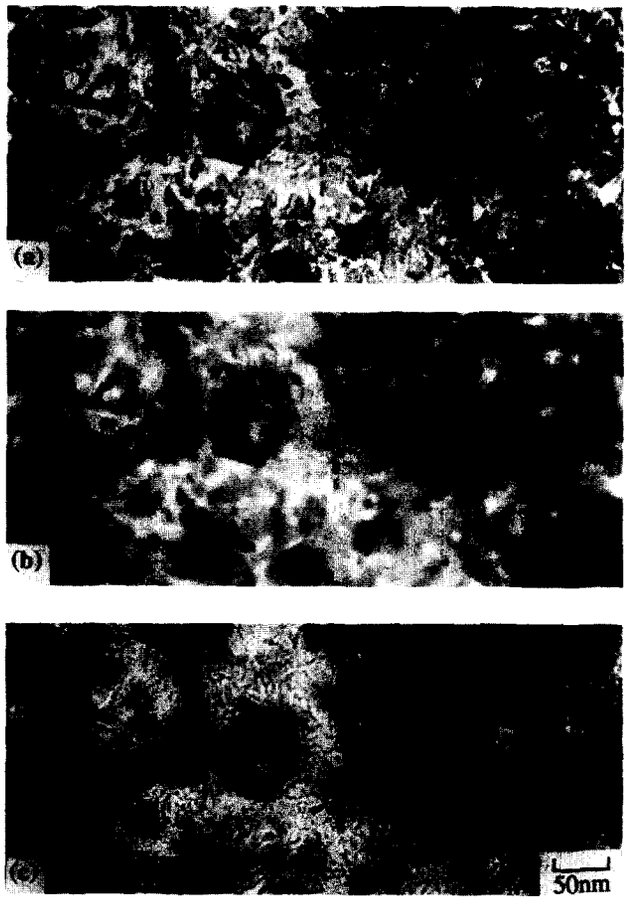

Fig. 3. TEM bright-field defocus images of a powder A compact sintered at 1250°C for 2 h: (a) under-focus (–220 nm), (b) near focus and (c) over-focus (2200 nm).

The mullite formation temperature of powder B was slightly lower than that of powder A or rather, more correctly, the rate of mullite formation at a given temperature and time was higher in powder B than in powder A. For instance, mullite formation was also observed in diphasic mixtures similar to powder A at temperatures as low as 1190°C but only after long-term isothermal heat treatment (24 h).[18] As the dissolution of alumina in the amorphous phase is rate-controlling for mullite formation and growth,[14,15] the higher rate of mullite formation in powder B can be explained by the smaller size of the alumina particles which results in higher rate of solubility at a given temperature. Therefore, more alumina becomes available for mullite formation.

3.2 Powder characteristics

The change in the surface area of each powder with calcination temperature is shown in Fig. 4. Both powders had a very high surface area which decreased with increasing calcination temperature. Assuming that powder A calcined at 550°C and powder B calcined at 940°C were mullite, the particle size of powders A and B calculated from their surface areas was 10 and 13 nm, respectively. However, both powders calcined at their respective temperature were not mullite (e.g. powder A calcined at 550°C should contain γ-Al_2O_3 and amorphous silica, both with different surface area and density). Therefore, the calculated particle size values should be considered as an approximation.

Figure 5 shows the particle size distribution of powders A and B, measured by the particle size analyser after milling for 24 h. The average particle size of both powders was ~ 2 μm. The large difference between the particle sizes calculated from the surface area and measured by the particle size analyser indicates agglomeration of nanometre-size particles.

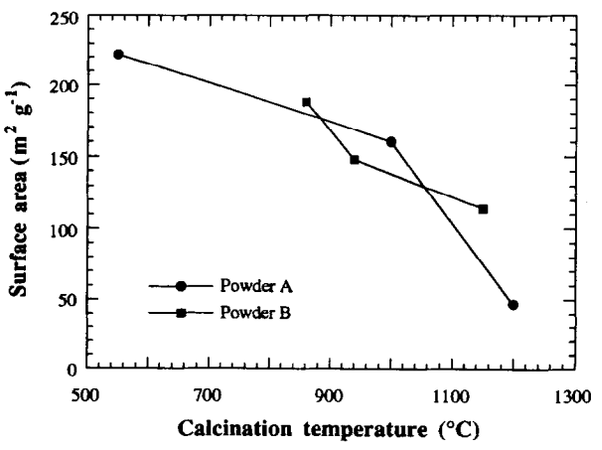

Fig. 4. Change in surface area of powders A and B with calcination temperature.

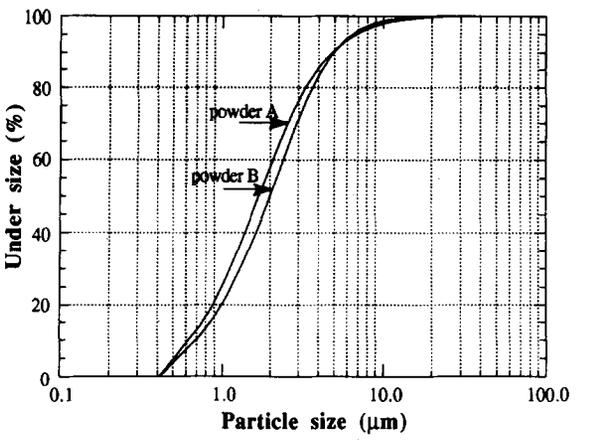

Fig. 5. Particle size distribution of powders A and B after milling in methanol for 24 h.

3.3 Sintering studies

3.3.1 Sintering of powder A

The compacts had a green density of ~45% after isopressing at 450 MPa. The effect of isothermal heat treatment on bulk density and open porosity of compacts prepared from powder A calcined at various temperatures is shown in Fig. 6. There was a sharp increase in density above 1100°C with the total elimination of open porosity at 1250°C. The location of the amorphous phase around the alumina particles and in the alumina particle grain junctions in Fig. 3 confirms that the sintering mechanism was the viscous flow of the amorphous phase. Therefore, the sharp increase in density can be attributed to the sharp decrease in the viscosity of the amorphous phase (silica-rich) with temperature. The increasing dissolution of alumina in amorphous silica also contributes to the decrease in viscosity.[19] The density of the compacts sintered at 1250°C was 3·01 g cm^{-3} (~95%). With the extensive formation of mullite above 1250°C (Fig. 2), the sintering almost stopped with only a further 3% increase in density between 1250 and 1600°C.

Optical microscope examinations of the polished surfaces of compacts sintered at 1250°C

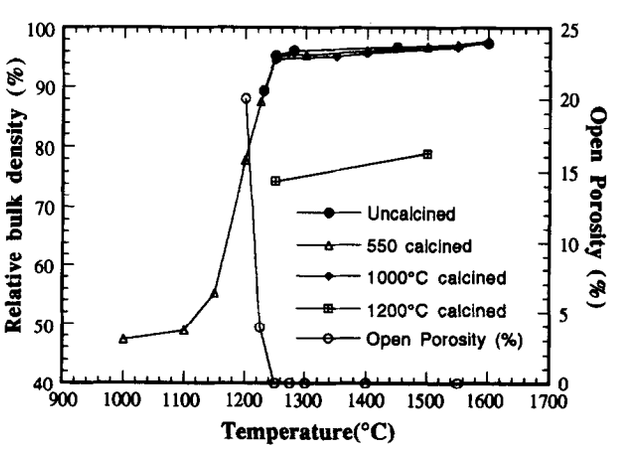

Fig. 6. Change in bulk density and open porosity of powder A compacts with sintering temperature. Sintering time is 2 h.

Fig. 7. TEM bright-field micrograph of a powder A compact sintered at 1250°C for 2 h showing the presence of micropores (some arrowed) scattered in the material.

Fig. 8. TEM bright-field micrograph of a powder A compact sintered at 1275°C for 2 h showing that pores present in the diphasic matrix are engulfed by mullite grains. White features inside the black mullite grain (M) are the pores.

showed almost no porosity although they were only 95% dense. This was due to the very small size of the pores (~30–35 nm with some as large as ~70 nm) as shown in Fig. 7, which were not resolvable in the optical microscope. The dense nature of the diphasic matrix around these pores suggests that they were the large pores inherited from the green compact. They are likely to be the result of some hard agglomerates which may be present in the powder. This is because the presence of hard agglomerates in powders causes the formation of inhomogeneous green compacts by creating two types of pores:[20] inter-agglomerate and intra-agglomerate (the pores between primary particles within the agglomerates), the latter being smaller than the former. This causes differential shrinkage and enlargement of inter-agglomerate pores since the intra-agglomerate pores are eliminated more rapidly or at a lower temperature due to their smaller size.[20] Then, the inter-agglomerate pores are eliminated, which need longer times and/or higher temperatures. It appears that these large pores could not be eliminated before mullite formation.

With the formation of mullite, the pores became engulfed by growing mullite grains as shown in Fig. 8. The mullite grain size was ~1·5 μm as shown in the figure. The elimination of the engulfed pores has to take place by diffusion of vacancies through the mullite lattice to reach the grain boundaries. Only ~3% pore elimination between 1250 and 1600°C indicates the difficulty of diffusion in the mullite lattice. Clearly, the elimination of the hard agglomerates will eliminate the large pores in the green compacts and full densification will become possible at 1250°C. For example, powders prepared by supercritical drying, which were proposed to be weakly agglomerated, sintered to ≥98% density at 1250°C.[8] If the large pores are not eliminated in the green state, high temperatures (≥1550°C) are needed for their removal.

The sintering behaviour of powder A calcined at various temperatures has already been included in Fig. 6, while Fig. 9 shows the effect of calcination temperature on sintered density at 1250°C and also on the overall weight loss of the pellets. As can be seen in these two figures, calcination temperatures up to 1000°C did not affect the sinterability of the powder but the weight loss decreased from 20% for the uncalcined powder to just over 5% for the 1000°C calcined powder. However, compacts prepared from powder calcined at 1200°C could only be sintered to 75% at 1250°C. This could be due to two reasons: (a) a decrease in the surface area of silica (as it is responsible for densification) and (b) formation of hard agglomerates during calcination which is unfavourable for packing. The occurrence of a substantial amount of sintering at 1200°C [in the

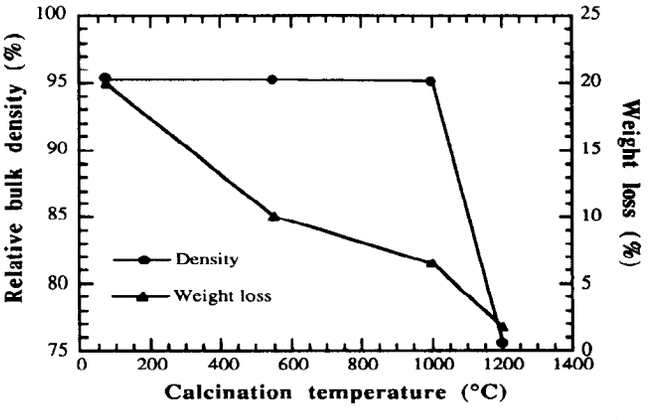

Fig. 9. Effect of calcination temperature of powder A on sintered density and weight loss of the compacts during sintering. Sintering is at 1250°C for 2 h.

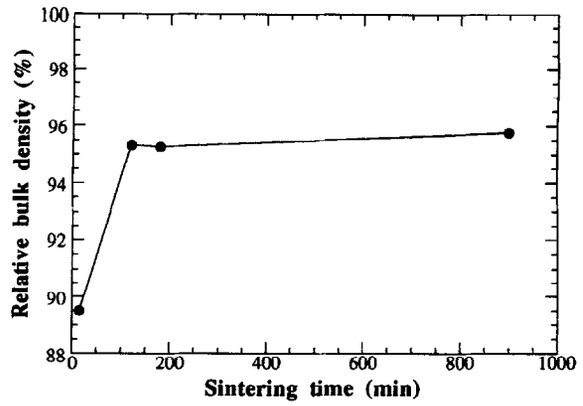

Fig. 10. Effect of sintering time on the sintered density at 1250°C.

powders calcined at ≤1000°C (Fig. 6)] is expected to cause extensive hard agglomerate formation during calcination at 1200°C. The density of 1200°C calcined compacts did not improve much on further increasing the sintering temperature to 1500°C, only 5% pore elimination taking place.

The effect of isothermal heat treatment time at 1250°C on sintered density is shown in Fig. 10. The densification at 1250°C takes place rather quickly and as high as 90% densification was achieved within 15 min. There was almost no difference in density between compacts sintered for 2 h and 15 h. This was not unexpected as mullite formation takes place after about 2 h and the densification mechanism changes into diffusion controlled. The diffusivities of related species in mullite at 1250°C are not expected to be significant.

3.3.2 Sintering of powder B

Figure 11 shows the effect of temperature on the relative bulk density of powder B compacts sintered for 5 h. There were two distinct stages of sintering. In the first stage, the densification was due to viscous flow as in powder A, where the compacts started to densify above 1100°C and showed a sharp increase in density with increasing temperature. However, since mullite formation in powder B takes place at a slightly lower temperature (~1200°C) than in powder A (1250°C), the viscous flow was disrupted at an earlier stage of sintering. Thus, powder B compacts could not be sintered to as high a density as powder A compacts by the viscous flow. The alumina–silica particle arrangement of powder B is also expected to have a detrimental effect on the densification rate in the first stage because silica surrounded by alumina is less effective for sintering due to disrupted connectivity of the viscous phase.[7] The maximum density achieved in this stage was only 70%. In the second stage (in the presence of mullite), the densification took place via solid-state diffusional processes. The temperature dependence of sintering was lower than the first stage (compare the slopes in both stages).

Figure 12 shows the effect of the magnitude of isopressure on green density and on sintered densities at various temperatures. Higher compaction pressures resulted in higher green densities and, in turn, higher sintered densities. However, the effect of green density became less pronounced with increasing temperature for a given sintering time. With the employment of isopressures as high as 1 GPa for compaction of the powder (which results in 58% green density), densities of up to 97% were achieved at temperatures as low as 1450°C.

The effect of calcination temperature on sinterability of powder B was reported earlier.[17] It was found that the sinterability of the powder was not affected when calcined up to a temperature below which there was no mullite formation (1100°C). However, if the powder was calcined at a high enough temperature to form mullite then the sinterability of the powder was reduced dramatically, demonstrating the improved sinterability of powder B when it does not contain mullite.[17] The improved sinterability of the green compacts not containing mullite compared with those made

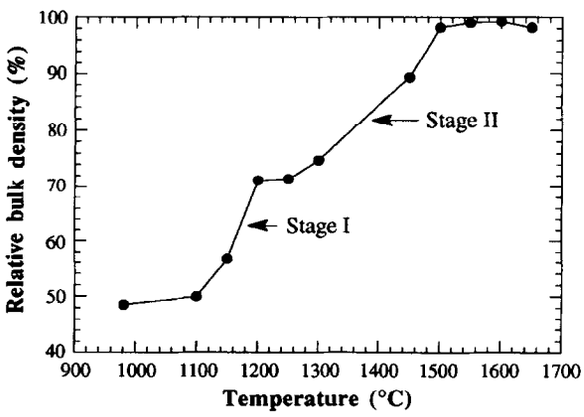

Fig. 11. Change in sintered density of powder B compacts with temperature. Sintering time is 5 h.

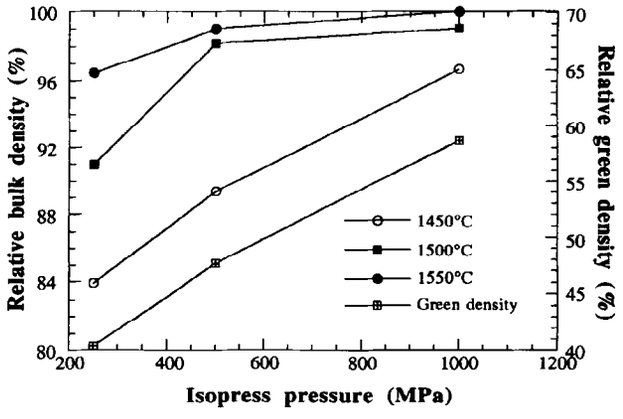

Fig. 12. Effect of isopress compaction pressure on green and sintered densities at various temperatures. Sintering time is 5 h.

from the crystalline mullite powder during solid-state sintering (stage II) (even though the mullite grain size is the same) can be attributed to the following factors :

(a) amorphous or weakly crystalline powders not containing mullite can be compacted to a smaller pore size and narrower pore size distribution due to their deformability at the contact point and due to their smaller size (i.e. better green microstructure),[21]

(b) limited viscous flow sintering causes an increase in density before solid-state sintering whereas crystalline mullite powder compacts do not show any densification up to 1400°C.[22–24]

The densification curves of powders A and B together with a fine crystalline mullite powder are compared in Fig. 13. Although powder B compacts had much more porosity to eliminate than powder A compacts by solid-state sintering (i.e. above 1250°C), powder B compacts sintered to near full density (>98%) at a lower temperature than powder A compacts. This was due to the fact that pores (engulfed inside mullite grains) in powder A compacts had to diffuse through 1·5 μm grain size mullite to reach the grain boundaries (Fig. 8), while the pores in powder B compacts were located at the multiple grain junctions as shown in Fig. 14. Even if they were located inside mullite grains, they would not have had to diffuse a long distance to reach the grain boundaries because the grain size was much finer (~0·15 μm) (Fig. 14). In addition, increased grain boundary area due to the fine grain size in powder B compacts should result in faster diffusion due to the availability of more diffusion channels. Entrapment of pores inside growing mullite grains during crystallization also appears to be the basic reason why 75% dense powder A compacts did not densify more than 5% between 1250 and 1500°C (Fig. 5).

The comparison of the sintering curves of powders A and B with that of the crystalline mullite powder in Fig. 13 shows that some 300–350°C and 150–200°C reductions in sintering temperature are possible with powder A and B, respectively, when they are reactively sintered.

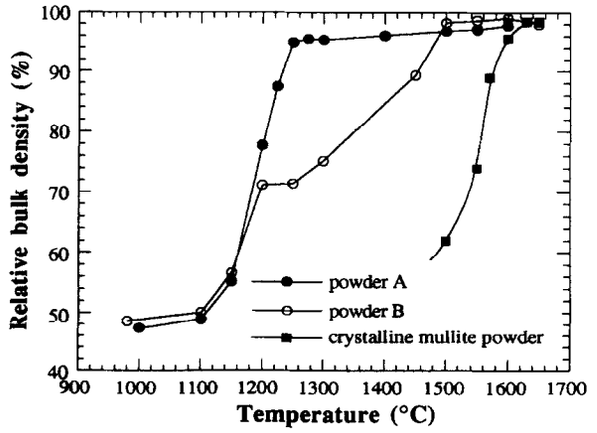

Fig. 13. Comparison of the sintering behaviour of powders A and B together with a crystalline mullite powder. Data for crystalline mullite powder are obtained from Ref. 24.

Fig. 14. TEM bright-field micrograph of a powder B compact sintered at 1450°C for 5 h (~95% dense). Arrows indicate the pores.

3.4 Stability of the fine microstructure of sintered powder B compacts

As shown previously, the grain sizes of mullite at low temperatures (where there is no appreciable grain growth) obtained from powder A and B were very different, mullite from powder B having a much smaller grain size. The only difference between the two powders was the size of the alumina particles used for preparation, these being much finer in powder B. Mullite formation from diphasic aluminosilicate mixtures occurs by self-nucleation from an intermediate amorphous aluminosilicate phase after reaching a critical alumina concentration,[25] i.e. alumina particles do not act as heterogeneous sites for mullite nucleation. After nucleation, growth of the nuclei takes place with no secondary nucleation. This means that the higher the nucleation frequency, the lower the mullite grain size. One possibility for the higher nucleation frequency in the presence of finer alumina particles could be that higher contact area between alumina and silica may cause many isolated regions reaching the critical nucleation concentration.

As powder B compacts could be sintered to high density (>95%) at low temperatures (~1450 or 1500°C for short times) when processed appropriately, grain growth of the mullite crystals was avoided (Fig. 14). Such a fine microstructure could be important in certain areas such as superplastic shaping and fibre making. Therefore, further experimental study was carried out to

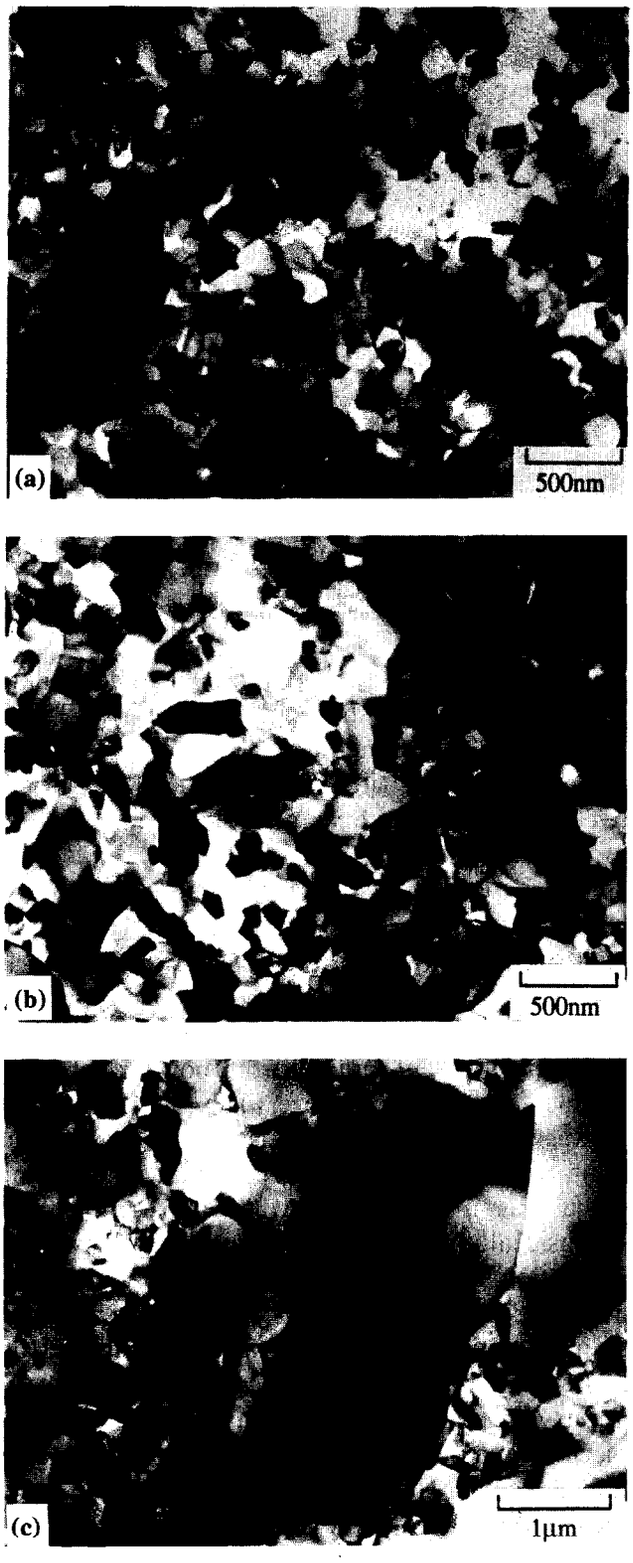

Fig. 15. TEM bright-field micrographs of powder B compacts (sintered at 1450°C for 5 h) after heat treatment at various temperatures for 120 h: (a) 1200°C, (b) 1300°C and (c) 1400°C.

measure the temperature limit of the stability of the fine grain size of the compact which was sintered at 1450°C for 5 h. This was done by conducting a constant period of 120 h heat treatment of the samples between 1200 and 1400°C.

Figure 15 shows TEM bright-field micrographs of mullite heat-treated between 1200 and 1400°C. As can be seen, the grain size did not appear to change up to 1300°C. This was confirmed by grain size measurements in TEM dark-field pictures using an image analyser. The average grain size of the as-sintered mullite (1450°C, 5 h) was ~135 nm, the smallest ever reported for dense polycrystalline mullite ceramics, and that of the 1200 and 1300°C heat-treated mullites was ~145 and 155 nm, respectively. However, at 1400°C although the grain size did not change much (~200 nm), extensive exaggerated grain growth was observed [Fig. 15(c)]. The extent of exaggerated grain growth was generally less than 1 μm, averaging about 0·5–0·7 μm, although in rare instances larger grains were also observed [Fig. 15(c)].

The occurrence of exaggerated grain growth during heat treatment at 1400°C must be due to the growth of very small amounts of larger grains which were already present in the as-sintered material (such as that indicated as A in Fig. 14). A large grain that is present in the matrix of fine grains will grow easily due to geometric (and thus free energy) considerations.[26]

Although fine and to a certain extent curved grain structure (Fig. 14) in powder B derived mullite in general aids grain growth, the stability of its fine microstructure up to ~1300°C can mainly be attributed to the low diffusivities in mullite at this temperature range as the rate of atom movement across the grain boundary is controlled by the diffusivity at grain boundaries.[26]

4 Conclusions

Homogeneously mixed precursor mullite powders were produced from boehmite–colloidal silica and aluminium sulfate–colloidal silica mixtures. The boehmite–silica mixture forms mullite at around 1250°C in the presence of δ-Al_2O_3 and an amorphous phase, and the aluminium sulfate–silica mixture forms mullite at 1200°C in the presence of γ-Al_2O_3 and an amorphous phase.

Sintering studies showed that powder derived from boehmite–silica mixture can be sintered at 1250°C to a high density (>95%) by viscous flow of the amorphous phase. Large pores, thought to be present in the green compact, could not be eliminated before mullite formation and formed the remaining ~5% porosity. With the formation of mullite the pores were engulfed by the growing mullite grains and, as a result, their elimination required high temperatures (≥1550°C). Calcination up to 1000°C did not affect the sinterability of the powder but caused a positive effect of reducing the weight loss during sintering. However, when calcined at 1200°C its sinterability was reduced dramatically.

Powder derived from aluminium sulfate–silica mixture could not be sintered to as high density as boehmite–silica mixture by viscous flow sintering as a result of the formation of mullite at an earlier stage which disrupts the viscous flow. However, sintering of the powder to almost full density was possible at around 1450–1500°C. Calcination temperatures up to 1100°C did not affect the sinterability of the powder. However, when calcined above the mullite formation temperature, its sinterability was reduced.

The nucleation frequency of mullite (and thus the grain size) appears to be governed by the size of the alumina component; the finer the alumina particle size, the higher the nucleation frequency and thus the smaller the mullite grain size. Dense and very fine grained mullite ceramics (<150 nm) can be produced from the powder derived from aluminium sulfate–colloidal silica mixture. The fine grain size was found to be stable up to temperatures of 1300°C or above on longer heat treatments.

References

1. Aksay, I. A. & Pask, J. A., Stable and metastable equilibrium in the system SiO_2–Al_2O_3. *J. Am. Ceram. Soc.*, **58** (1975) 507–12.
2. Boch, P., Chartier, T. & Rodrigo, P. D. D., High purity mullite ceramics by reaction sintering. In *Ceramic Transactions, Vol. 6, Mullite and Mullite Matrix Composites*, ed. S. Somiya, R. F. Davis & J. A. Pask. American Ceramic Society, Westerville, OH, 1990, pp. 353–74.
3. Sacks, M.D., Bozkurt, N. & Scheiffele, G.W., Fabrication of mullite and mullite matrix composite by transient viscous sintering of composite powders. *J. Am. Ceram. Soc.*, **74** (1991) 2428–37.
4. Miao, X. & Marquis, P.M., Vitreous sintering of heterocoagulated alumina silica sols. *Nanostructured Mater.*, **1** (1992) 31–6.
5. Komarneni, S., Suwa, Y. & Roy, R., Application of compositionally diphasic xerogels for enhanced densification: the system Al_2O_3–SiO_2. *J. Am. Ceram. Soc.*, **69** (1984) C155–6.
6. Sonuparlak, B., Sol–gel processing of infrared transparent mullite. *Adv. Ceram. Mater.*, **3** (1988) 263–7.
7. Fahrenholtz, W. L., Smith, D. M. & Cesarano III, J., Effect of precursor particle size on the densification and crystallization behaviour of mullite. *J. Am. Ceram. Soc.*, **76** (1993) 433–7.
8. Jeng, D.-Y. & Rahaman, M. N., Sintering and crystallization of mullite powder prepared by sol–gel processing. *J. Mater. Sci.*, **28** (1993) 4904–9.
9. Kara, F., Processing and characterisation of mullite based ceramics. PhD thesis, University of Cambridge, Cambridge, UK, 1994.
10. Hulling, J. C. & Messing, G. L., Surface chemistry effects on homogeneity and crystallization of colloidal mullite sol–gels. In *Ceramic Transactions, Vol. 6, Mullite and Mullite Matrix Composites*, ed. S. Somiya, R. F. Davis & J. A. Pask. American Ceramic Society, Westerville, OH, 1990, pp. 221-9.
11. Okada, K., Otsuka, N. & Somiya, S., Review of mullite synthesis routes in Japan. *Am. Ceram. Soc. Bull.*, **70** (1991) 1633–40.
12. Wei, W.-H. & Halloran, J. W., Transformation kinetics of diphasic aluminosilicate gels. *J. Am. Ceram. Soc.*, **71** (1988) 581–7.
13. Li, D. X. & Thomson, W. J., Kinetic mechanisms for mullite formation from sol–gel precursors. *J. Mater. Res.*, **4** (1990) 1963–9.
14. Hulling, J. C. & Messing, G. L., Epitactic nucleation of spinel in aluminosilicate gels and its effect on mullite crystallization. *J. Am. Ceram. Soc.*, **74** (1991) 2374–81.
15. Sundaresan, S. & Aksay, I. A., Mullitisation of diphasic aluminosilicate gels. *J. Am. Ceram. Soc.* **74** (1991) 2388–92.
16. Clarke, D. R., On the detection of thin intergranular films by electron microscopy. *Ultramicroscopy*, **4** (1979) 33–44.
17. Kara, F. & Little, J. A., Sintering of pre-mullite powder obtained by chemical processing. *J. Mater. Sci.*, **28** (1993) 1323–6.
18. Wei, W.-H. & Halloran, J. W., Phase transformation of diphasic aluminosilicate gels. *J. Am. Ceram. Soc.*, **71** (1988) 166–72.
19. Bansal, N. P. & Doremus, R. H., *Handbook of Glass Properties*. Academic Press, Orlando, FL, 1986.
20. Sacks, M. D. & Pask, J. A., Sintering of mullite containing materials: II, Effect of agglomeration. *J. Am. Ceram. Soc.*, **65** (1982) 70–7.
21. Kamiya, H., Suzuki, H., Takahiro, T. & Jimbo, G., Ultra-high pressure cold isostatic pressing — low temperature sintering of alkoxide derived mullite precursor powders. *Ceram. Eng. Sci. Proc.*, **13** (1992) 563–70.
22. Mizuno, M. & Saito, H., Preparation of highly pure fine mullite powder. *J. Am. Ceram. Soc.*, **72** (1989) 373–82.
23. Mitachi, S., Matsuzawa, M., Kaneko, K., Kanzaki S. & Tabata, H., Characterisation of SiO_2–Al_2O_3 powders prepared from metal alkoxides. In *Ceramic Transactions, Vol. 6, Mullite and Mullite Matrix Composites*, ed. S. Somiya, R. F. Davis & J. A. Pask. American Ceramic Society, Westerville, OH, 1990, pp. 274–85.
24. Kumazawa, T., Ohta, S., Kanzaki, S. & Tabata, H., Influence of powder characterisation on microstructure and mechanical properties of mullite ceramics. In *Ceramic Transactions, Vol. 6, Mullite and Mullite Matrix Composites.*, ed. S. Somiya, R. F. Davis & J. A. Pask. American Ceramic Society, Westerville, OH, 1990, pp. 401–11.
25. Aksay, I. A., Dabbs, D. M. & Sarikaya, M., Mullite for structural, electronic and optical applications. *J. Am. Ceram. Soc.*, **74** (1991) 2343–58.
26. Kingery, W. D., Bowen, H. K. & Uhlmann, D. R., *Introduction to Ceramics*. Wiley Interscience, New York, 1976.